

Numerical Simulation and Parameter Optimization of the Inside Intake and Outside Pressing Particle Collector

LU Zhongliang^{1,2,3,4}, CHEN Weifeng¹, XU Yahui¹, WANG Hongli^{5*} and ZHENG Guosheng⁶

1. School of Safety Science and Engineering, Henan Polytechnic University, Henan, Jiaozuo 454003, China

2. The Collaborative Innovation Center of coal safety production of Henan Province, Henan, Jiaozuo 454003, China

3. Key Laboratories of Gas Geology and Gas Control, Henan Polytechnic University, Henan, Jiaozuo 454003, China

4. Collaborative Innovation Center of Central Plains Economic Region for Coalbed /Shale Gas of Henan Province, Henan, Jiaozuo 454003, China

5. School of Mathematics and Information Science, Henan Polytechnic University, Henan, Jiaozuo 454003, China

6. Department of Engineering Sciences, NEUT, Yonggi-do 907, Korea,

Received 2 March 2015; Accepted 2 November 2015

Abstract

The issue of high dust concentration and the difficulty of head-on collection were investigated in this study. The theory of gas-solid two-phase flow was used to conduct numerical simulations on the air flow and dust concentration of the inside intake and the outside pressing particle collector using the FLUENT 6.3.26 software. The best optimization scheme was obtained by analyzing the simulation results of the air flow and dust concentration. Results indicated that when the diameter of the external cavity was 700 or 900 mm, the working surface of the working environment was not effectively improved. In comparison, when the diameter of the external cavity was optimized to 800 mm, most of the dust was trapped in the working face, and the working environment was significantly improved.

Keywords: dust, inside intake and outside pressing particle collector, parameter, numerical simulation, optimization scheme

1. Introduction

The production of Chinese coal energy increases yearly; in fact, the national coal production reached 3.7 billion tons in 2013. Coal production is thus growing rapidly. However, the safety of underground production should be ensured. Coal dust is a major hazard in the production process. Apart from threatening the health of mine workers, the dust that encounters heat can cause an explosion. Such an explosion can lead to serious accidents and major losses for the state and enterprises as well as threaten social stability and harmonious development. Based on incomplete statistics, large coal dust explosions have killed more than 1,000 people in recent years. Dust not only causes explosions but also leads to miners suffering from pneumoconiosis, a lung disease caused by the long-term intake of dust and gas [1–4].

The downhole production process, mainly from dust accumulated during the excavation of coal crushing and unreasonable ventilation, expands the scope of dust pollution. Ventilation is widely used to prevent dust hazards and to reach standard safety procedures for roadway dust concentration. Therefore, the focus of prevention and control of dust hazards involves three aspects, namely, rational optimization (roadheader), ventilation, and a dust-removal device; face ventilation; and dust collection or the maximum dust collected. Worker safety and management systems

improved early in foreign countries, and their employees have a strong sense of security compared with those in China. Therefore, there are more studies on coal dust hazard in foreign countries than in China. Precipitators are widely used in some of the major coal-producing countries abroad. Dust blowers, wet fiber precipitators, small cyclones, and other equipment are used in the United States. In Russia, wet vibrating precipitators and vacuum pumps are used in the roadheader, shearer or steeply inclined coal seam, return airway, and other places. In Germany, dry bag filters are used in the vicinity of a crusher at the transshipment point and roadheader [5]. Meanwhile, in China, a series of studies has been conducted on filters. Professor Xu Lin from Beijing University of Technology has developed a new and efficient self-excited precipitator. The Chongqing coal science branch has developed a new generation of precipitators that can be used with other comprehensive roadheaders that obtain good dust-removal effects [6]. Based on external pressure pumping dust collector patents, the current study optimizes the external cavity dimensions of the dust collector and conducted numerical simulations using FLUENT. Thereafter, the simulated data are analyzed to optimize the removal efficiency of the dust collector cavity size.

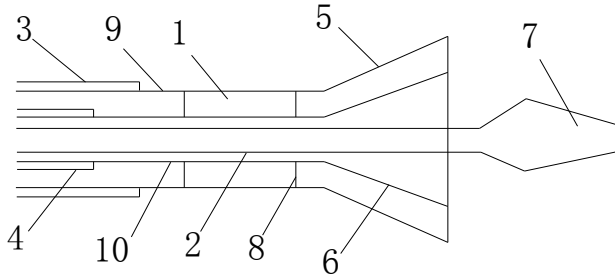
2. Structure and working principles of the external pressure pumping dust collector

The simple push-in or draw-out structure is commonly used; however, the collection of the dust cannot reach a reasonable

* E-mail address: wanghongli@hpu.edu.cn

amount. On the one hand, the simple push-in dust collector only has a simple injection and dilution function and is unable to remove dust. Moreover, it can cause large ranges of pollution. On the other hand, the lift of the simple draw-out dust suction is short because the fan layout is unreasonable, usually causing eddy currents and expanding the scope of dust pollution [7]. Based on the traditional dust-collection methods, this new method has been improved using a newly invented external pressure pumping dust collector, which has received national patents.

The external pressure pumping dust collector initially focuses on the minimum range and then concentrates on removing dust using the flow fields inside and outside the cavity. The exhaust and pushed fan tubes are installed in the internal and external cavities, respectively. The cutting arm is set in the internal cavity, which thereafter becomes the digging machine drill and opens both inside and outside the chambers connected to the bell. The cavity and the outer part of the exhaust fan are connected by the pipeline. The outer chamber through the exhaust pipe is connected to the push-in fan. Dust is gathered within the lumen using the external cavity jet and the lumen suction flow, after which the dust is processed in a precipitator [8–9]. The structure is shown in Figure 1.



1. external cavity 2. lumen cavity 3. exhaust pipe 4. intake pipe 5. outside trumpet
6. inside trumpet 7. drill of the roadheader 8. pillar 9. outer barrel 10. inner barrel
Fig.1. Cavity structure of the inside intake and outside pressing particle collector

The cavity includes external and lumen cavities. The external cavity is the dust outlet, and the lumen cavity is the dust inlet. The exhaust and intake pipes are both full pipes, and for easy calculation, both are excluded in the computational domain. The length of the external cavity is 2 m, and the gap size between the external cavity and the cutting arm is 0.2 m (with 800 mm cavity). The lengths and angles of the outside and inside trumpets are both 0.4 m and 45°, respectively. The sizes of the drill of the roadheader are simplified to 3 m in the computational domain. The length of the outer barrel is 4 m. The length and the gap size of the inner barrel is 0.2 m. The diameter of the lumen cavity is 600 mm, and the length of the lumen cavity is 1.5 m.

3. Numerical simulation of the cavity of the inside-intaking and outside-pressing particle collector

3.1 Mathematical model

The discrete phase model is a model of continuous and discrete phase interactions (dust in the roadway is a discrete phase, and air is a continuous phase) using motion and trajectory calculations of flow-field particles. The flow regime is turbulent flow, and the type of study is an unsteady state problem. Usually, the flow field of the continuous phase is calculated first, and then the jet of the discrete phase is created. Finally, the variable flow field trajectories are used to calculate the discrete phase particles through the

discrete phase model [10–12]. Several control equations were obtained based on kinetic theory of the discrete phase and the conservation laws of the continuous phase. These equations are described below.

The continuity equation for the gas is given by

$$\frac{\partial \rho}{\partial t} + \frac{\partial(\rho u)}{\partial x} + \frac{\partial(\rho v)}{\partial y} + \frac{\partial(\rho w)}{\partial z} = 0 \quad (1)$$

where ρ is the fluid density, t is the time, and u, v, w are the components of velocity.

The equation for conservation of momentum is expressed as

$$\frac{\partial u_i}{\partial t} + \overline{u_j} \frac{\partial \overline{u_i}}{\partial x_j} = \frac{1}{\rho} \frac{\partial}{\partial x_j} (\overline{\sigma_{ij}} - \rho \overline{u_i u_j}) + f_i \quad (2)$$

where $\overline{\sigma_{ij}}$ is the normal surface force, $-\rho \overline{u_i u_j}$ is the Reynolds stress (expressed as a ripple effect of the averaged flow), and f_i is the effect of gravity.

In the K-epsilon of the turbulence model, the equation of K is given by

$$\rho \frac{\partial k}{\partial t} + \frac{\partial}{\partial x_j} (\rho v_j k) = \frac{\partial}{\partial x_j} \left[\frac{\mu}{\sigma_k} - \frac{\partial k}{\partial x_j} \right] + G - \rho \epsilon \quad (3)$$

The equation of ϵ is expressed as

$$\rho \frac{\partial \epsilon}{\partial t} + \frac{\partial}{\partial x_j} (\rho v_j \epsilon) = \frac{\partial}{\partial x_j} \left[\frac{\mu_t}{\sigma_\epsilon} - \frac{\partial \epsilon}{\partial x_j} \right] + \frac{\epsilon}{k} (c_1 G - c_2 \rho \epsilon) \quad (4)$$

where G is the turbulence kinetic energy term, $G = \mu_t \left(\frac{\partial v_i}{\partial x_j} + \frac{\partial v_j}{\partial x_i} \right) \frac{\partial v_i}{\partial x_j}$;

μ_t is the turbulent viscosity coefficient, $\mu_t = \frac{c_\mu \rho k^2}{\epsilon}$; and

$c_1, c_2, c_\mu, \sigma_k, \sigma_\epsilon$ are the empirical constants, with $c_1=1.44, c_2=1.9, c_\mu=0.09, \sigma_k=1.0, \sigma_\epsilon=1.2$.

The discrete phase dust equation conservation equation is given by

$$\frac{du_p}{dt} = F_D(u - u_p) + \frac{g_x(\rho_p - \rho)}{\rho_p} + F_x \quad (5)$$

where $F_D(u - u_p)$ is the unit mass of drag force of the discrete phase, $g_x(\rho_p - \rho) / \rho_p$ represents the subtracts of gravity and buoyancy of the discrete phase, and F_x represents the other forces that can be ignored.

3.2 Geometric model and parameter settings

Based on the measured data of the west tunneling working face of the Lu'an mine, the tunnel section had a length of 3.5 m, width of 3.5 m, and height of 3 m. The diameter of the inner cylinder was 600 mm, which was suitable for the cutting arm. Based on the data from the previous experiments, the size of the external cylinder was simulated separately by three sets of data, namely, 700, 800 and 900 mm, respectively. The system was simplified for convenient calculation, and the length of the external cavity and lumen were both 2.4 m (including the trumpet). The geometric

models of the different diameters of the external cylinder were created using GAMBIT, as shown in Figure 2. The grid was then divided, and the boundary conditions were defined. Finally, the models were imported into the FLUENT software, and the boundary conditions and dust source parameters were set [13–14]. These conditions and parameters are shown in Tables 1 and 2.

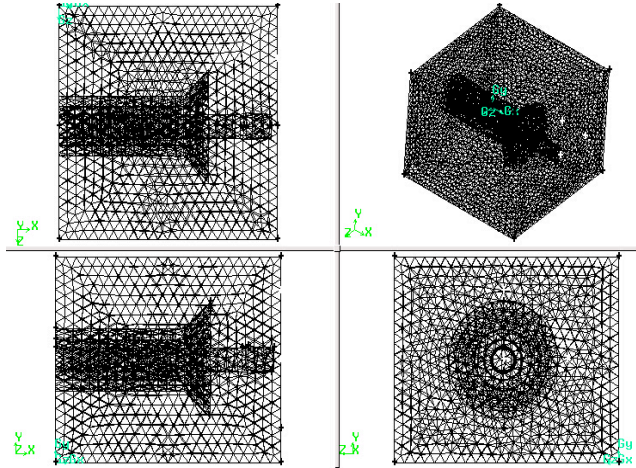


Fig. 2. Meshing of the cavity of the inside intake and outside pressing particle collector

Table 1. Main parameters of the boundary conditions

Boundary conditions	Parameter setting
Export wind speed of roadway (m/s)	0.35
Inner barrel absorb wind speed (m/s)	8
Outer barrel mouth blowing wind speed (m/s)	15
Hydraulic diameter (m)	3.2
Turbulence intensity (%)	2.5
Inlet boundary types	Velocity-Inlet
Outlet boundary types	OUTFLOW

Table 2. Main parameters of the dust source

Particle source	Parameter setting
Size distribution	Rosin–Rammmler distribution
Minimum size (m)	1.0×10^{-6}
Maximum particle size (m)	1.0×10^{-4}
Initial velocity (m/s)	0
Dust concentration (kg/m^3)	2.5×10^{-3}
Mass flow rate (kg/s)	9.2×10^{-3}

The boundary type of the heading face was the wall; those of the roadway roof, floor, container wall and coal wall were all wall, that of the tunnel outlet was the outflow; those of the outer barrel inlet and inner barrel outlet were the velocity-inlet; and those of the outer barrel outlet and the inner barrel inlet were the interval. The computational domain was the working face, and the model selected had a size of $3.5 \text{ m} \times 3.5 \text{ m} \times 3 \text{ m}$. The distance between the center of the inner cylinder diameter and the floor of the roadway

was set at 1.8 m, whereas that between the trumpet-shaped section and the heading working surface was set at 2.4 m. The tunnel out of the heading face was the export wind speed in the computational domain. The inner barrel absorb wind speed was used in the lumen cavity, and the entrance velocity of the inner barrel was negative. The outer barrel mouth wind speed was used in the external cavity, and the entrance velocity of the outer barrel was positive.

The hydraulic diameter is calculated using the equation

$$L = 4S / l \quad (6)$$

where S (m^2) is the flow cross-sectional area, and l (m) is the flow cross-sectional perimeter.

The turbulence intensity is calculated based on the type (7). This empirical formula is obtained under the inferential reasoning of the predecessor, which is given by

$$I = 0.16 \times \text{Re}^{-\frac{1}{8}} \quad (7)$$

where Re is the Reynolds calculated by the hydraulic diameter, ($\text{Re} = \frac{\rho v d}{\mu}$).

The mass flow rate is calculated using the equation

$$\text{Mass flow rate} = c \cdot v \cdot S \quad (8)$$

where c is the dust concentration in kg/m^3 , v is the wind velocity in m/s, and S is the cross-sectional area in m^2 .

All walls were assumed to be insulated and had no sliding; the pressure gradient perpendicular to walls was 0. The grid interval size was 0.15. If the grid size is smaller, then the analogue result is more sophisticated for the entire geometry model. Given its complex structure, using the Tgrid meshing method is relatively more successful than other methods when it comes to carrying out the separation. Without the need for user intervention methods of the Tgrid, the grid structure can change into a large grid density, which reduces the time of mesh, thus guaranteeing the quality of the grid.

The convergence criterion is absolute convergence. When the residual is below 0.001, it is convergence. The time step is 0.1 s, and the number of time steps is 5000. The coupling frequency discrete phase model is 10, which is the discrete phase for each iteration step corresponding to the iterative 10-step continuous phase, and the number of calculated steps is set to 5000.

4 Results and analysis of the numerical simulation

Based on the main parameters of the actual measured underground tunneling face, the cavity sizes of the 700, 800 and 900 mm cavities were simulated to obtain the flow motion in the dust cavity and the change in the concentration of discrete particles. The evaluations to this study are as given below.

4.1 Simulation of the 700 mm cavity

Figure 3 shows that in the outside air under pressure from the external cavity flow duct face, dust particles are surrounded by air flows as they pass through the duct lumen and are finally collected in the dust collector. When the cavity diameter is 700 mm, the air from the external cavity is

found after injection, but the formation of a local small-scale surround area is unable to collect a significant amount of dust cutting points. The diagram of dust concentration changing with time shows that the dust concentration remains at $1.0 \times 10^{-3} \text{ kg/m}^3$ in 250 s, which gradually decreases to 350 s.

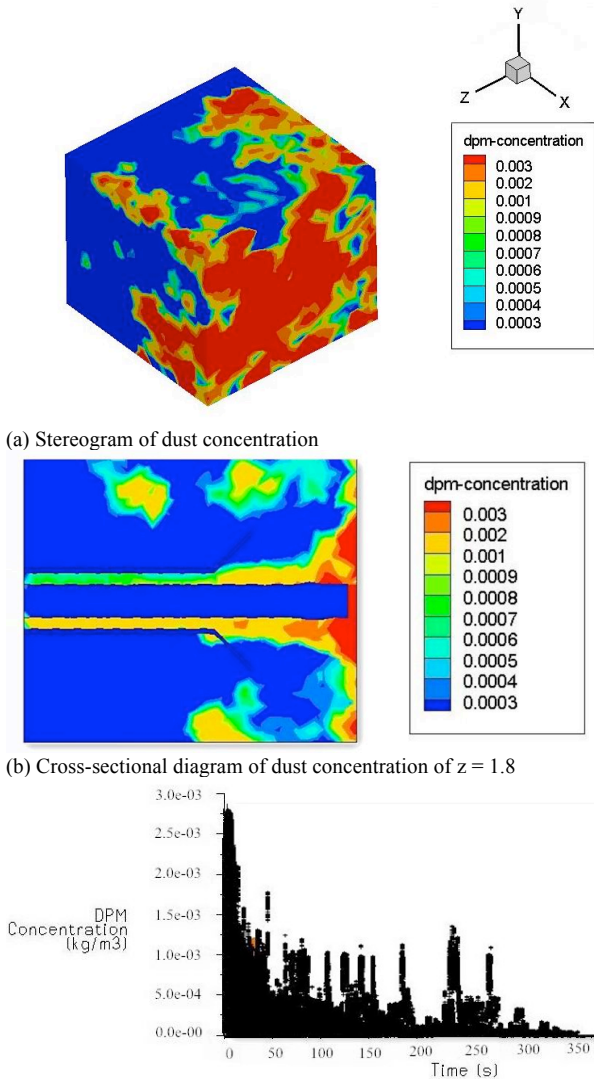


Fig. 3. Changes of dust concentration in the working surface

4.2 Simulation of the 800 mm cavity

Figure 4 shows that the surrounding area significantly increases compared with that in Figure 3 by increasing the diameter of the external cavity duct. In the area near the cutting point, the flow field in the external pressure jet and the flow field inside the vacuum suction influence each other, forming inside the pumping region surrounded by external pressure. From the analysis of the changes in dust concentration, dust concentration from the beginning is $3.0 \times 10^{-3} \text{ kg/m}^3$, gradually stabilizing until it remains at a low concentration range after 50 s. The face cutting point produces a significant amount of dust particles flowing through the lumen of the duct, which are then collected in the dust collector.

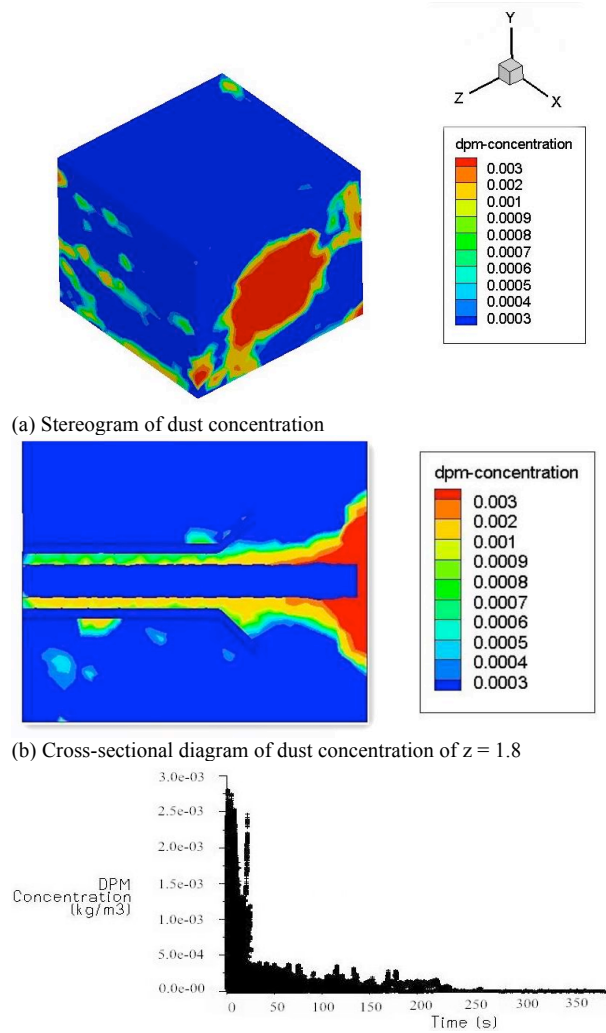
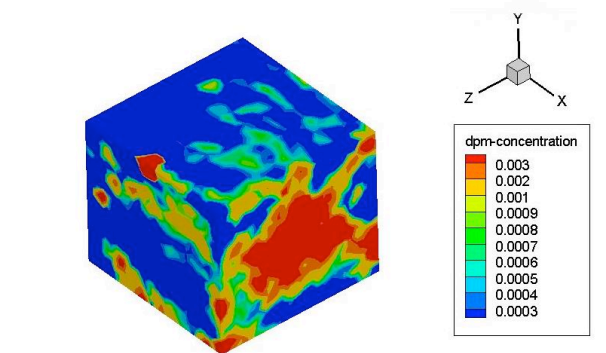


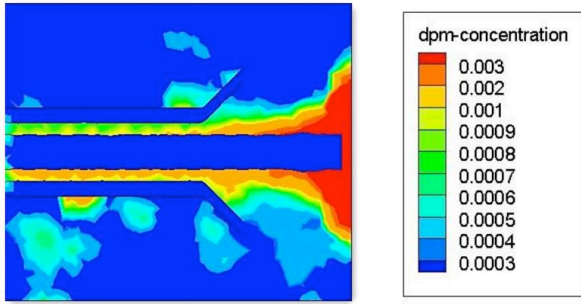
Fig. 4. Changes of dust concentration in the working surface

4.3 Simulation of the 900 mm cavity

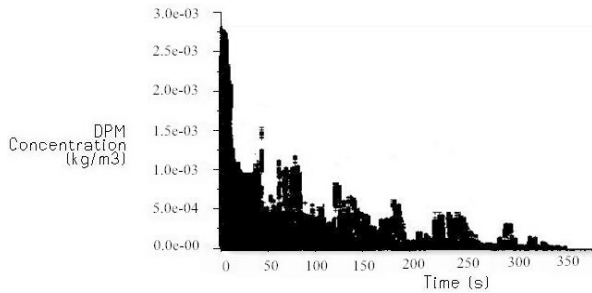
Based on Figures 3 and 4, the tube diameter of the external cavity is expanded, as shown in the results in Figure 5. Figure 5 shows that the area enclosed by the airflow further expands. However, part of the airflow flows outward along with the tunnel roof and the bottom plate because of the changes in the external cavity size. The dust concentration in the face also quickly drops from $3.0 \times 10^{-3} \text{ kg/m}^3$ to $5.0 \times 10^{-4} \text{ kg/m}^3$ within 200 s. However, the accumulation of a large amount of dust particles curled up by the top floor flow would seriously threaten the safety of the workplace personnel.



(a) Stereogram of dust concentration



(b) Cross-sectional diagram of dust concentration of $z = 1.8$



(c) Diagram of dust concentration changing with time

Fig. 5. Changes in dust concentration found in the working surface

4.4 Selection of the simulation program

In summary, when the duct diameter of the external cavity is 700 mm, the working environment cannot be effectively improved. In comparison, when it is 800 or 900 mm, the dust concentration effectively decreases, and the dust particles are quickly collected within a short period of time. When the diameter of the outer cylinder is 900 mm, a significant amount of dust spreads out with the air movement through the roof and the floor, and this movement is affected by the height of the cylinder. Such air movement can affect safe production and human health. Therefore, the

external cavity duct with an 800 mm diameter is the best option to maximize external pressure in the dust-extraction device. This finding acquired through field measurement indicates that the proposed device can better control the dust concentration, compared with a pressure-type dust and extraction device, in the rock roadway west tunnel located in the coal mine in the Shanxi Lu'an Group tunneling face. Furthermore, the device effectively reduces the dust hazards of the underground tunneling face.

5. Conclusions

(1) Dust generated by a cutting point is in motion. The proposed device can control the flow of dust production and point movement by optimizing the size of its structure, which can effectively reduce the concentration of dust in the tunneling face.

(2) The size of the external cavity for trapping dust is vital. When the diameter of the external cavity is 800 mm, the dust trapping effect is satisfactory, and the dust concentration in a wider range of working surfaces is reduced while ensuring a safe working environment. When the diameter of the external cavity is 700 or 900 mm, the face of the working environment cannot be effectively improved because of the influence of the diameter of the cavity and height of the subject.

(3) The results of the simulation coincide with the patented product, which achieves the desired effect. These results can serve as a reference for controlling dust control in underground work.

Acknowledgements

This work was supported by the Foundation for National Natural Science (No.51174109).

References

1. SI Rongjun, "Research Status and Development Trend of Gas and Coal Dust Explosion". *Mining Safety & Environmental Protection*, 41 (1), 2014, pp.72-75.
2. LI Run-qiu, SHI Shi-liang, NIAN Qi-feng, "Research on Coalmine Gas Accident Rules in China in Recent Decade". *China Safety Science Journal*, 21(9), 2011, pp.143-151.
3. WEI Qiang, "Hazard of mine dust and its prevention and cure". *Journal of Henan and Technology*, (11), 2014, pp.49-50.
4. QU Shuang-yi, HUANG Wen-li, LI Jin-hong, "Research for the actuality and analysis for countermeasures of the occupational disease in coal mine". *Chinese Journal of Coal Industry Medicine*, 15(4), 2012, pp.569-570.
5. LI Xin-yu, ZHANG He-jun, ZHANG De-chao, "Development and experimental research of new mining wet dust collector". *Shandong coal Science and Technology*, (9), 2014, pp.79-82.
6. XIAO Wen-yu, "Present situation and Prospect of coal mine dust control technology in China". *Science & Technology information*, (4), 2014, pp.226-227.
7. MENG Jun, "Research on Technology and Management of Air-water Spraying Dust Suppression in Fully Mechanized Coal Face". *China University of Mining Technology Press*, 2013.
8. LU Zhong-liang, "Inside Inhaling and Outside Pressing Particle Collector". *Baiteng network*, <http://so.5ipatent.com/PatentDetails.aspx?patentID=49fd15f2-b855-4b20-a3c0-3e1981d5ada1&patentClass=1>, 2009.
9. LU Zhong-liang, FAN Xiao-li, XIAO Ya-ning, "Experimental and Numerical Analysis of Flow Field in Inside Inhaling and Outside Pressing Particle Collector". *China safety science journal*, 18(10), 2008, pp.99-103.
10. WANG Xiao-zhen, JIANG Zhong-an, "WANG Shan-wen, Numerical simulation of distribution regularities of dust concentration during the Ventilation process of coal roadway driving". *Journal of China Coal Society*, 32(4), 2007, pp.386-390.
11. CHEN Ju-shi, JIANG Zhong-an, YANG Bin, "Numerical simulation of spatial dust concentration distribution regularities in crushing chamber". *Journal of China Coal Society*, 37(11), 2012, pp.1865-1870.
12. LIU Yi, JIANG Zhong-an, CAI Wei, "Site measurement and digital simulation of dust density distribution in fully mechanized longwall coal mining face". *Coal Science and Technology*, 34(4), 2006, pp.80-82.
13. ZHANG Jian-zhuo, ZHU Tian-zi, GAO Meng, "Parameter Optimization and Numerical Simulation of Dust-collecting and Dedusting System with Air Curtain in Fully Mechanized Excavation Face". *China safety science journal*, 21(4), 2011, pp.128-131.
14. YAO Yu-jing, CHENG Wei-min, NIE Wen, "Numerical Simulation of Dust Concentration Distribution in a Fully Mechanized Heading Face". *Mining Safety & Environment Protection*, 38(3), 2011, pp.21-23.
15. ZHOU Jun-bo LIU Yang, "FLUENT 6.3 Flow analysis from entry to the master". *China Machine Press*, 2012.